

# Applying the Water Vapor Radiometer to Verify the Precipitable Water Vapor Measured by GPS

Ta-Kang Yeh<sup>1,\*</sup>, Jing-Shan Hong<sup>2</sup>, Chuan-Sheng Wang<sup>1</sup>, Tung-Yuan Hsiao<sup>3</sup>, and Chin-Tzu Fong<sup>2</sup>

<sup>1</sup> Department of Real Estate and Built Environment, National Taipei University, New Taipei City, Taiwan

<sup>2</sup> Meteorological Information Center, Central Weather Bureau, Taipei, Taiwan

<sup>3</sup> Department of Information Technology, Hsing Wu University, New Taipei City, Taiwan

Received 16 October 2012, accepted 14 October 2013

---

## ABSTRACT

Taiwan is located at the land-sea interface in a subtropical region. Because the climate is warm and moist year round, there is a large and highly variable amount of water vapor in the atmosphere. In this study, we calculated the Zenith Wet Delay (ZWD) of the troposphere using the ground-based Global Positioning System (GPS). The ZWD measured by two Water Vapor Radiometers (WVRs) was then used to verify the ZWD that had been calculated using GPS. We also analyzed the correlation between the ZWD and the precipitation data of these two types of station. Moreover, we used the observational data from 14 GPS and rainfall stations to evaluate three cases. The offset between the GPS-ZWD and the WVR-ZWD ranged from 1.31 to 2.57 cm. The correlation coefficient ranged from 0.89 to 0.93. The results calculated from GPS and those measured using the WVR were very similar. Moreover, when there was no rain, light rain, moderate rain, or heavy rain, the flatland station ZWD was 0.31, 0.36, 0.38, or 0.40 m, respectively. The mountain station ZWD exhibited the same trend. Therefore, these results have demonstrated that the potential and strength of precipitation in a region can be estimated according to its ZWD values. Now that the precision of GPS-ZWD has been confirmed, this method can eventually be expanded to the more than 400 GPS stations in Taiwan and its surrounding islands. The near real-time ZWD data with improved spatial and temporal resolution can be provided to the city and countryside weather-forecasting system that is currently under development. Such an exchange would fundamentally improve the resources used to generate weather forecasts.

Key words: Global positioning system, Zenith wet delay, Water vapor radiometer, Rainfall

Citation: Yeh, T. K., J. S. Hong, C. S. Wang, T. Y. Hsiao, and C. T. Fong, 2014: Applying the water vapor radiometer to verify the precipitable water vapor measured by GPS. *Terr. Atmos. Ocean. Sci.*, 25, 189-201, doi: 10.3319/TAO.2013.10.14.01(A)

---

## 1. INTRODUCTION

Since its development, Global Positioning System (GPS) technology has been widely used in many fields. The application of GPS technology to the field of meteorology is called GPS Meteorology (GPS/Met). The primary purpose of this work was to utilize the delay effect of the GPS satellite signal, which is caused by Earth's atmosphere, to derive useful atmospheric information and ultimately contribute to the development of atmospheric science, meteorology, and other related fields. Many examples from European and American countries have suggested that performing near real-time atmosphere monitoring using the GPS tracking network can positively contribute to long-term climate monitoring and

short-term weather forecasting (Aguado and Burt 2009; Solomon 2011). Currently, there is an increasing demand for weather forecasting, especially emergent weather forecasting. By utilizing continuous observation from a GPS signal, the dynamic variations of precipitation in the troposphere can be observed. The near real-time continuous nationwide precipitation data, which feature high precision, as well as high spatial and temporal resolution, can be used in meteorology research to improve the ability to forecast emergent weather. GPS offers some advantages when compared with meteorological radar and radiosonde, which are traditionally used in weather forecasting. Meteorological radar can measure the spatial distribution of raindrops, but it cannot measure water vapor distribution. This drawback greatly weakens its usage for weather-forecast warnings. The radiosonde

---

\* Corresponding author  
E-mail: bigsteel@mail.ntpu.edu.tw

is a single-use piece of equipment that has low temporal resolution; its typical sampling rate is twice daily. Conversely, because ground-based GPS is inexpensive, it can be densely distributed. GPS technology can provide nearly real-time, highly precise, and continuously varying Precipitable Water Vapor (PWV) data across a wide coverage area (Liou et al. 2001). This ability is very important for improving the short-term weather-forecast capability, especially for thunderstorm forecasting and numerical weather-forecast models. Currently, the ground-based GPS network of the National Oceanic and Atmospheric Administration (NOAA) of the United States can automatically estimate the variation of PWV above the network surface every 30 min (NOAA 2013). The Japanese GPS network, consisting of more than 1000 stations, has also been used in functional ground-based GPS meteorological applications (Shoji 2009).

Although GPS can facilitate the ability to make highly precise measurements of the phases of carrier waves for navigation, the error caused by the atmosphere has drawn increasing attention. These errors arise due to ionospheric and tropospheric delays. For the ionospheric delay, the error can be reduced using dual-frequency observation or simultaneous observations of the differential method (Leick 2004; Yeh et al. 2008). The tropospheric delay consists of two components: the dry component (caused by the temperature and pressure variations of the dry air, which change the refractive index of the air) and the wet component (caused by the uneven distribution of water vapor, which causes the signals to refract). The dry delay exists when the atmospheric temperature and pressure are constant, and the wet delay also exists when the water vapor is evenly distributed. The former component can be precisely calculated using ground pressure detection (Chen et al. 2011). However, the latter component cannot be easily corrected because of the uneven distribution and instability of the atmospheric water vapor. Although the wet delay of the troposphere is much smaller than the dry delay, the uncertainty of the troposphere wet delay introduces a lack of predictability into high-precision GPS applications (Solheim et al. 1999; Yeh et al. 2006). The upper limit of water vapor in the atmosphere is only 4%. Of this water vapor, 75% occurs between the surface and an altitude of 4 km. In addition, 50% of this water vapor is distributed between the surface and at an altitude of 2 km (Ruddiman 2007). Nearly all of the water vapor (approximately 99%) occurs in the troposphere. Finding an effective solution for the troposphere delay would increase the precision of GPS positioning and could also be used to derive the PWV of the atmosphere to provide a near real-time ability to forecast weather.

The atmospheric delay along the path of electromagnetic waves is largely unknown. Therefore, many models estimate delay values for electromagnetic waves in the atmosphere using ground meteorological data, the elevation angle, and the azimuth angle. These delay values differ

based on the empirical model from which they are derived, and the ground-meteorology empirical models are primarily used to estimate the Zenith Wet Delay (ZWD). When it comes to the other part, the zenith dry delay, we also use an empirical model to correct this kind of error. The precision of the zenith dry delay from an empirical model can be less than 1 mm (Ifadis and Savvaidis 2001). However, due to the uneven distribution of water vapor at high altitudes, many questions remain regarding the estimation of ZWD using ground-empirical models (Mendes and Langley 1999). In a study of Sweden and Finland, the differences between Water Vapor Radiometer (WVR) and GPS observations of the PWV are about 1 - 2 mm, based on field measurements for three months (Emardson et al. 1998). The accuracy of absolute PWV can also be estimated from GPS observations (Tregoning et al. 1998). They found that GPS, radiosonde, and WVR estimates of PWV differ by 1.4 mm between any two kinds of observations, with a bias of 0.2 mm. Moreover, Liou et al. (2000) suggested that the most accurate GPS estimates of PWV were achieved when the GPS analysis contains station separations of more than 2000 km. In this study, we used fourteen ground-based GPS stations to derive ZWD information. We then compared the ZWD data with observational data from two WVRs to verify the accuracy of the GPS-ZWD data. The results of this comparison can be used in industrial fields and to calculate atmospheric PWV. In the future, these results can provide supporting information that can be used in weather forecasting and in environmental monitoring.

## 2. THEORY OF THE TROPOSPHERE DELAY

The troposphere primarily influences the GPS signal in two ways. The propagation speed of the signal is slowed down relative to that of a vacuum, and the signal path is bent rather than straight; both of these effects are caused by refraction along the propagation path. For the former effect, the refraction index of the troposphere is larger than that of a vacuum, thereby causing a time delay known as the speed delay or propagation-time delay. For the latter effect, because the refraction index varies with altitude, the propagation path is bent and the signal is also delayed. These two types of delays, the speed delay and the path delay, are discussed in the following section.

### 2.1 Speed Delay

The effect of the propagation-time delay can be estimated from the refractive index  $n$ . The relationship between the speed in a vacuum and that in a medium can be expressed as follows:

$$V_M = \frac{V_v}{n} \quad (1)$$

in which  $V_v$  is the signal speed in a vacuum, and  $V_M$  is the signal speed in the medium. The refractive index of the medium changes along the propagation path, because of temperature and pressure variations. Therefore, the index is a function of the path, and the speed delay  $D_v^{Trop}$  due to the different speeds is expressed as follows:

$$D_v^{Trop} = \int [n(s) - 1] ds \quad (2)$$

## 2.2 Path Delay

The path delay is due to the oblique angle between the direction of the wave and the direction of the variations in  $n$ . Because the refractive index of the atmosphere changes according to the atmospheric height, an electromagnetic wave that travels through the atmosphere will generally have a bent rather than a straight path. The bent path is longer than the straight line, the path is elongated between the satellite and the receiver. The path delay  $D_p^{Trop}$  is expressed as follows:

$$D_p^{Trop} = S - G \quad (3)$$

in which  $S$  and  $G$  represent the straight and bent paths, respectively. In summary, the troposphere delay  $D^{Trop}$  can be expressed as follows:

$$D^{Trop} = D_v^{Trop} + D_p^{Trop} = \int [n(s) - 1] ds + (S - G) \quad (4)$$

In Eq. (4),  $\int [n(s) - 1] ds$  is the effect of the speed delay, and  $(S - G)$  is the effect of the bent path. In general, the  $(S - G)$  delay is less than 1 cm when the elevation angle is greater than  $15^\circ$ , and it only represents 0.1% of the total delay (Bock and Doerflinger 2001). Therefore, this delay can be neglected. The primary factor that causes the apparent longer path is the variation of refractive index as a function of height in the atmosphere. According to Eq. (4), the zenith tropospheric delay  $\Delta L_{Trop}^Z$  is as follows:

$$\Delta L_{Trop}^Z = \int_H^\infty [n(z) - 1] dz = 10^{-6} \int_H^\infty N dz \quad (5)$$

where the refractive index  $N$  can be expressed as follows:

$$N = \left( k_1 \frac{P_d}{T} \right) Z_d^{-1} + \left( k_2 \frac{e}{T} + k_3 \frac{e}{T^2} \right) Z_w^{-1} \quad (6)$$

$N$  is a function of temperature, pressure, and water vapor pressure;  $P_d$  is the dry air pressure;  $e$  is the water-vapor pressure;  $T$  is the absolute temperature;  $k_1$ ,  $k_2$ , and  $k_3$  are constants;  $Z_d$  is a dry air compression factor; and  $Z_w$  is a water-vapor compression factor. Finally, from Eq. (6), we derive the following:

$$\begin{aligned} \Delta L_{Trop}^Z &= D_{Trop,h}^Z + D_{Trop,w}^Z \\ &= 10^{-6} \left\{ \frac{k_1 R}{g_m M_d} P_s + \int_H^\infty \left[ \left( k_2 - k_1 \frac{M_w}{M_d} \right) \frac{e}{T} + k_3 \frac{e}{T^2} \right] dz \right\} \end{aligned} \quad (7)$$

in which  $D_{Trop,h}^Z$  is the dry delay,  $D_{Trop,w}^Z$  is the wet delay,  $R$  is a molar gas constant,  $g_m$  is the mass center of the vertical air column,  $M_d$  is the molar weight of the dry air,  $M_w$  is the molar weight of the water vapor, and  $P_s$  is the surface atmospheric pressure. In Eq. (7),  $\frac{k_1 R}{g_m M_d} P_s$  (expressed as  $\Delta L_h^Z$ ) is the zenith hydrostatic delay, or the dry delay, which can be calculated by measuring the total surface atmospheric pressure; the term  $\int_H^\infty \left[ \left( k_2 - k_1 \frac{M_w}{M_d} \right) \frac{e}{T} + k_3 \frac{e}{T^2} \right] dz$  (expressed as  $\Delta L_w^Z$ ) is the wet delay, which can be calculated when the atmospheric temperature and water vapor pressure are known. Typically, the zenith signal delay caused by a neutral atmosphere is approximately 2.3 m. When the signal elevation angle is  $5^\circ$ , the delay caused by a neutral atmosphere can reach approximately 25 m (Chen and Herring 1997).

Because the GPS signals pass through media with unknown refractive indexes, surface meteorological parameters (temperature, humidity, and pressure) are used to model the troposphere. To date, researchers have developed several tropospheric delay-correction models. Among these models, the most well-known is the Niell model (Niell 1996). For the Niell model, no meteorological parameter is required. The dry component is calculated from the latitude, the station elevation, and the day of the year. The wet component can be obtained by entering the latitude of the station. These terms can be expressed as follows:

$$D_{dry}^{Trop}(\epsilon) = \frac{1}{\sin \epsilon + \frac{a_{dry}}{\sin \epsilon + c_{dry}}} + \frac{1 + \frac{a_{dry}}{b_{dry}}}{1 + c_{dry}} \quad (8)$$

$$\left[ \frac{1}{\sin \epsilon} - \frac{1 + \frac{a_{ht}}{b_{ht}}}{1 + c_{ht}} \right] \times \frac{H}{100}$$

$$\left[ \frac{1}{\sin \epsilon + \frac{a_{ht}}{\sin \epsilon + c_{ht}}} \right]$$

$$D_{wet}^{Trop}(\epsilon) = \frac{1}{\sin \epsilon + \frac{a_{wet}}{\sin \epsilon + c_{wet}}} + \frac{1 + \frac{a_{wet}}{b_{wet}}}{1 + c_{wet}} \quad (9)$$

in which  $\varepsilon$  is the elevation angle of the satellite,  $H$  is the elevation,  $a_{ht} = 2.53 \times 10^{-5}$ ,  $b_{ht} = 5.49 \times 10^{-3}$ , and  $c_{ht} = 1.14 \times 10^{-3}$  km. The hydrostatic delay calculated from the Niell model has been verified many times, and it is known to be accurate to 1 mm or less (Yeh et al. 2012). Using the standard atmosphere status and the empirical meteorological model to replace the observation data from the ground station produces favorable results (Bock and Doerflinger 2001). However, this analysis is only applicable to long-term data analyses in which the impact of emergent weather events has been reduced. When data are analyzed over many years, climatic variations can be observed and detected. However, when data are analyzed over the course of a few hours or a few days, the particular daily atmospheric conditions will lead to variations in the daily coordinate calculation results.

To convert the ZWD to PWV according to the definition of precipitable water vapor, the relationship between the ZWD ( $\Delta S_w$ ) and PWV ( $P_w$ ) is as follows:

$$P_w = \Pi \times \Delta S_w \quad (10)$$

in which  $\Pi$  is the scale factor and can be calculated as follows:

$$\Pi^{-1} = 10^{-6} [\rho R_w (k_3/T_m + k'_2)] \quad (11)$$

in which  $k_2$  and  $k_3$  are the experimental constants for the atmospheric refraction, such that  $k_2 = 64.79$  K hPa<sup>-1</sup>,  $k_3 = 3.766 \times 10^5$  K<sup>2</sup> hPa<sup>-1</sup>, and  $k'_2 = k_2 - k_1 M_w/M_d = 16.52$  K hPa<sup>-1</sup>. The molar mass of water vapor ( $M_w$ ) is 18.015 g mol<sup>-1</sup>, such that  $R_w = R/M_w = 461.524$  J kgK. The scale factor  $\Pi$  is related to the temperature; it changes with the latitude, the height of the station, the season, and the weather. Therefore, the method used to determine the temperature is very important. Davis et al. (1985) posted a solution and defined the weighted average temperature as follows:

$$T_m = \int_{h_s}^{\infty} \frac{e}{T} dh / \int_{h_s}^{\infty} \frac{e}{T^2} dh \quad (12)$$

in which  $e$  is the water vapor pressure and  $T$  is the atmospheric temperature (in Kelvin). Using radiosonde data that have been collected for many years, Bevis et al. (1994) derived the following linear relationship between the weighted average temperature  $T_m$  and the surface temperature  $T_s$ :  $T_m = 70.2 + 0.72 T_s$ . The ZWD can then be converted to PWV.

### 3. DATA COLLECTION AND PROCESSING

In this study, we choose the plum rain, the typhoon,

and the long-duration (three-month) seasons for the case studies. Three datasets were used: GPS, precipitation and WVR data. The processing steps and the methods that were used for these datasets are explained below.

#### 3.1 GPS Data

The GPS data in this study were obtained from the following 14 GPS stations: YMSM, GS10, SHJU, CAOT, TACH, PKGM, SINY, KDNM, YILN, SOFN, TMAM, LANB, MZUM, and KMMN (Fig. 1). The Bernese 5.0 software program, developed by the University of Bern in Switzerland, was used to analyze the GPS data. First, we calculated the precise coordinates of the 14 GPS stations from daily solutions using the three months data. Because the standard deviations of the 3-D coordinates were less than 5 mm, we calculated the average coordinates of each of these 14 GPS stations. Furthermore, the ZWD was obtained based on the assumption that the coordinates of the ground points are fixed. During the process of differential calculation, the orbit error and the clock error of the satellite were corrected using the IGS precise ephemeris. The ionosphere delay error was eliminated using the L3 linear combination (Leick 2004; Yeh et al. 2013). To avoid eliminating the desired ZWD during the elimination of the common error while performing the differential calculation, we used the method of long-baseline static relative positioning to ensure that the ZWD was obtained with high accuracy (Liou et al. 2000). Because the separations of GPS stations were more than 2000 km, the propagation paths through the atmosphere to each station were assumed independent. When we used the double-difference method to obtain the ZWD, it remained very close to absolute value (Tregoning et al. 1998). Moreover, to increase the accuracy of the ZWD calculation, the ocean-tide loading correction was applied, and the NAO.99b model was used to achieve the optimal correction effect (Yeh et al. 2011).

Another important issue was the selection of the reference station. We tested various combinations of reference stations and distances; these stations were TSKB (Japan), GUAM (Guam), BJFS (Beijing), DAEJ (Korea), and YUSN (Taiwan). After comparing the ZWD measured by WVR, TSKB (Japan) was chosen as the reference station because it produced the best result. At distances greater than 2000 km, the atmospheric properties can be treated as uncorrelated between any two locations. By increasing the baseline distance between the reference and calculation stations, atmospheric information can be preserved during the differential calculation, thereby achieving a more accurate ZWD. Furthermore, due to the adequacy of the data and the comprehensive error correction, the sampling frequency of the ZWD was once per hour or 24 times per day per station. In other words, the temporal resolution of the GPS-deduced ZWD was 1 hr.

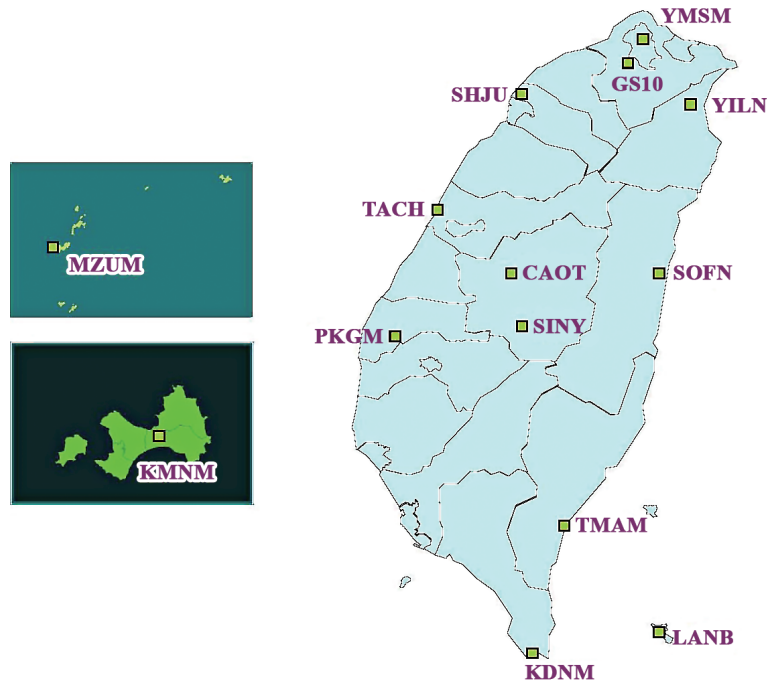


Fig. 1. The distribution of the GPS observation stations.

### 3.2 Rainfall Data

To match the locations of the GPS stations, the 14 precipitation stations from the Central Weather Bureau (CWB) rainfall database located nearest to each of the GPS stations were selected (Chutzuhu, Taipei, Hsinchu, Taichung, Wuqi, Chiayi, Alishan, Hengchun, Yilan, Hualien, Taitung, Lanyu, Matzu, and Kinmen). The time resolution of these data was also 1 hr, yielding 24 samples per station per day. Due to the 8-hr time difference between the GPS time and the precipitation time (Taiwan local time), the precipitation time was converted to GPS time prior to analysis.

### 3.3 WVR Data

This study utilized the WVP-1500 radiometer, which was developed by the Radiometrics Corporation in the US; this is a passive WVR that has five observation wavebands between 22 and 30 GHz. Its observation range can reach up to a 10-km water vapor cross section, and the single observation time is less than 10 sec. This instrument can also be used to measure surface temperature, pressure, and relative humidity. Figure 2 shows an architectural diagram of the Radiometrics WVP-1500, which was equipped with an Azimuth Drive component. The Radiometrics WVP-1500 can provide measurements at various azimuth angles by tracking GPS satellites through the GPS satellite ephemeris to scan every observable satellite. Therefore, the PWV liquid water content can be measured to calculate the wet delay caused by the atmosphere. Moreover, this instrument includes a

Rain Effect Mitigation component, which includes Superblower and Hydrophobic Radome modules; these modules prevent measurement error due to the adhesion of water drops to the WVR. On a technical level, the PWV measured by the WVR should be more accurate than GPS-measured PWV. The WVR data used in this study were provided by the Ministry of the Interior (MOI), Taiwan government. Five frequencies (22.2, 23.0, 23.8, 26.2 and 30.0 GHz) are used for measuring the brightness temperatures. The “TIP Calibrations” method is designed to accompany the regular measuring work for calibrations. According to the official procedure of WVR maintenance from MOI, the measurements of “TIP Calibrations” (called  $T_{nd}$  values) are averaged from all the daily measurements every season. These averages are applied for updating the  $T_{nd}$  values in the configuration file for five frequencies. Therefore, we used the WVR-measured PWV as a standard in this study to verify the accuracy of the GPS-calculated ZWD. Due to the cost constraints of WVR, however, GPS is a more economical, real-time, wide-coverage observation method.

The two WVRs were installed at the satellite tracking stations of Yangmungshan (YMSM) and Beigang (PKGM). The distance between the GPS antenna and the WVR was around 3 m, and the elevation of these two instruments was almost the same. Figure 3 shows the location of the GPS antenna and the WVR at station YMSM. There are four types of output files (level 0, level 1, level 2 and tip) from WVRs. The voltages for the measured parameters are recorded in the level 0 file. The level 1 file contains brightness temperatures for the each channel (five frequencies). The ZWD



Fig. 2. Architectural diagram of the Radiometrics WVP-1500 radiometer.

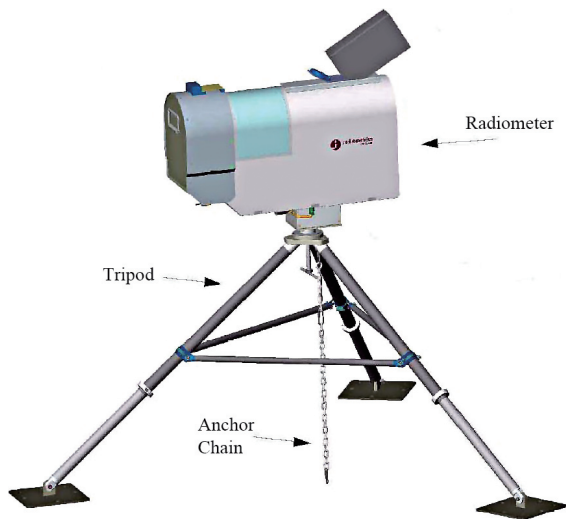


Fig. 3. The location of GPS antennas and WVR at station YMSM.

value is recorded in the level 2 file, and, theoretically, is not the real raw measurement from the WVR machine. The retrievals (level 2) are produced using the level 1 data and the neural network files specified in the configuration. The neural network files, including the conversion coefficient, are based on over 10 years of data from all radiosonde stations in the Taiwan area, and are created by the company called “Radiometrics Corporation”. The original data from the WVR included the date, time, surface temperature, pressure, and relative humidity. The resolution between observations was less than 10 sec. Therefore, the volume of WVR data was very large. After modifying the sampling rate of each set of WVR, GPS and precipitation data, the correlation analysis was then performed with the GPS-ZWD and the precipitation data.

## 4. CASE STUDY AND RESULT ANALYSIS

### 4.1 Case 1: Plum Rain Season

The plum rain season occurs each May and June in Taiwan. The precipitation of the plum rain season accounts for 1/4 of the total annual precipitation, and it is the major water-supply source in Taiwan. However, excessive precipitation can also cause disasters. The features of the plum rain season can vary between years. Even meteorologists admit that the predictability of rainfall during the plum rain season is low, and that the weather is highly variable (Kueh et al. 2009). We therefore chose to study the plum rain season, and analyzed the relationship between the precipitation observed during the season and the GPS-ZWD values. A time period that included the Modified Julian Day (MJD) 53887 - 53900 (June 1 - 14, 2006) was chosen for this case study. Based on the information provided on the CWB website, most of the areas in Taiwan experienced continuous rainfall during MJD 53887 - 53899. The central and southern areas experienced torrential and extremely torrential rain, respectively. Some disasters occurred as a result of the continuous heavy or torrential rainfalls. During this period, the most notable rainfalls occurred between MJD 53896 and 53897. Starting at MJD 53900, the weather front began to move north. The weather in Taiwan shifted to the summer type, which is controlled by the Pacific High and involves higher daily temperatures. The rain system changed primarily in response to thermal convection, which developed after noon (CWB 2011).

This case included 14 stations. We first chose stations Yangmungshan and Beigang as examples, because GPS and WVR data are available for both stations. In Fig. 4, the red line represents the wet delay measured by the WVR, the green line the wet delay calculated from the GPS data, the blue line the surface precipitation, and the gray line represents the surface humidity. We determined that the ZWD measured by the WVR (referred to as WVR-ZWD) and the ZWD calculated from GPS data (referred to as GPS-ZWD) displayed the same trend (Fig. 4). The correlation coefficient between the GPS-ZWD and the WVR-ZWD data was 0.96, which shows that these two time series are highly correlated. Furthermore, by calculating the differences between the GPS-ZWD and WVR-ZWD estimates, and then averaging the absolute values of these differences, the average discrepancy between the two ZWDs was 1.19 cm. This preliminary result verified the reliability of the ZWD calculated from the GPS data. The trends of the GPS and WVR results were found to be consistent. Minor systematic errors exist between the two results.

The result for station PKGM is shown in Fig. 5. The differences between the WVR-ZWD and GPS-ZWD values were relatively larger than for station YMSM. The correlation coefficient was only 0.77: a much poorer correlation

than that observed at station YMSM. Upon further analysis, we found that the results of the red line (WVR-ZWD) and the green line (GPS-ZWD) are broadly similar. However, they do not coincide with each other from MJD 53895 - 53896, which were the two days with heavy rainfall. During these two days, the average precipitation was more than 20 mm hr<sup>-1</sup>, which is considered to be torrential rain. Therefore, the observed ZWD should have synchronously increased. However, the red line (measured by WVR) decreased while the green line (calculated from the GPS data) increased. This result suggests that the GPS is more reliable than the WVR during heavy rainfall. The strong rainfall period was the primary reason for the low correlation coefficient. If we excluded this period, the correlation coefficient between the GPS-ZWD and the WVR-ZWD values was 0.9, which is highly correlated. Moreover, by using the method used for station YMSM to calculate the absolute values of the differences, the average discrepancy between the GPS-ZWD and WVR-ZWD values was 1.42 cm. This result suggests that a relatively larger systematic error exists between the GPS-ZWD and WVR-ZWD data when the rainfall intensity is large. Such a phenomenon could be related to the measurement error caused by water drops adhering to the surface of the WVR during periods of heavy rainfall. Although the WVR is equipped with the Rain Effect Mitigation component, GPS data are more reliable than WVR data during heavy rainfall.

#### 4.2 Case 2: Two Typhoons

This case encompassed MJD 53950 - 53960 (August 3 - 13, 2006). Seven typhoons occurred in August of that year. We chose the Bopha and Saomai typhoons as examples. Typhoon Bopha formed in the sea east of Taiwan. The maxi-

mum wind speed near the typhoon center was 23.0 m s<sup>-1</sup>. The landing point was in eastern Taiwan. The CWB activated the typhoon landing alarm on MJD 53955. The intermittent, large rainfall brought by Bopha (the total precipitation was approximately 250 mm in the mountain area) caused crop damage. Typhoon Saomai formed in the sea southwest of Guam. The maximum wind speed near the typhoon center was 48.0 m s<sup>-1</sup>. The CWB activated the typhoon landing alarm on MJD 53956. Due to the rapid speed of Saomai, the warning time was short. Moreover, the cloud cluster was dense and concentrated within the storm circle. Only northern Taiwan, which was passed by the storm circle, experienced relatively strong wind and intermittent rainfalls during the morning of MJD 53957. The CWB cancelled the alarm in the afternoon on MJD 53957.

The data used in this case study were also derived from the GPS and precipitation stations. Stations YMSM and PKGM also produced the WVR data. Figure 6 shows similar trends to those observed in Case 1. At station YMSM, the ZWD calculated from the GPS data and the ZWD measured by the WVR showed the same trend with a correlation coefficient of 0.93 and an average discrepancy of 2.47 cm. Both the correlation coefficient and the discrepancy were worse than the values calculated for the plum rain season case. This result may have been caused by the severe weather changes that occurred during the typhoon period, which decreased the accuracy of the ZWD calculation. Figure 6 clearly shows that the ZWD increased rapidly when the typhoon was approaching and decreased rapidly as the typhoon left. The hourly precipitation reached its maximum on MJD 53957. The GPS-ZWD and WVR-ZWD values reached peak levels simultaneously. Two days after the typhoon (MJD 53959), ZWD rapidly decreased to its minimum during the period.

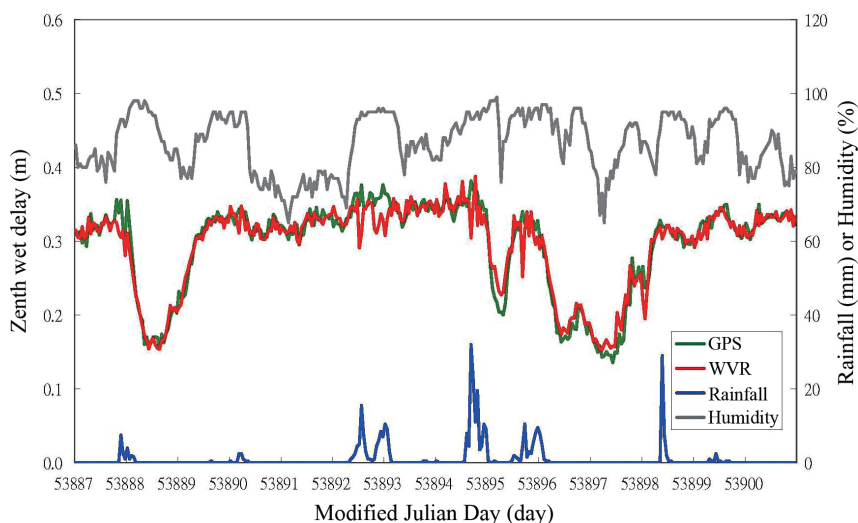


Fig. 4. The GPS-ZWD, WVR-ZWD, relative humidity, and precipitation data from station YMSM during the plum rain season.

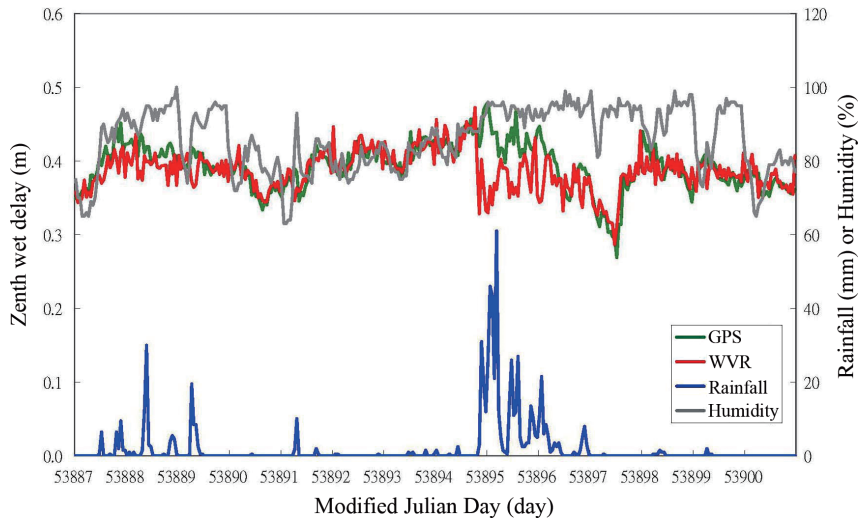


Fig. 5. The GPS-ZWD, WVR-ZWD, relative humidity, and precipitation data from station PKGM during the plum rain season.

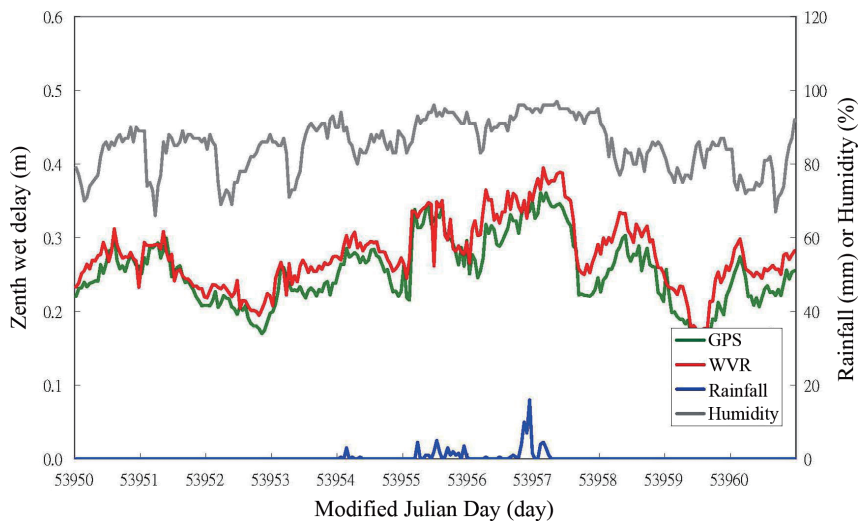


Fig. 6. The GPS-ZWD, WVR-ZWD, relative humidity, and precipitation data from station YMSM during the typhoon period.

We next analyzed the data from station PKGM. Figure 7 shows that after the first typhoon began to affect Taiwan (MJD 53955), the data from the WVR became erratic. Further investigation revealed that the abnormal data were caused by a servomotor failure. The WVR uses the servomotor to rotate the equipment to track the GPS satellites. However, the servomotor failed because of the strong wind produced by the typhoon, causing the measured data to become incorrect. Prior to the servomotor failure, the GPS-calculated ZWD and the WVR-measured ZWD values displayed the same trend. When the data after MJD 53955 were excluded, the correlation coefficient between the GPS-ZWD and the WVR-ZWD measurements was calculated to be 0.85. The average discrepancy was 2.67 cm. Both of these parameters were worse than those calculated in the plum rain season case, which was similar to the results for YMSM.

This result again suggests that the accuracy of the ZWD is reduced during the typhoon period. Figure 7 also shows that the GPS-ZWD values increased rapidly when the two typhoons were closest to Taiwan (MJD 53957 and 53957). After the typhoons, the GPS-ZWD values decreased rapidly. One day after the typhoons (MJD 53958), the GPS-ZWD measurements decreased rapidly to the minimum values for the period.

#### 4.3 Case 3: Long Duration

The long-duration case used three months of data, from MJD 53826 to 53917 (April - June, 2006). We used the same stations as in the previous two cases. Figure 8 shows the results for station YMSM. We can see that the long-duration and short-duration cases (Case 1 and 3) are similar. ZWD

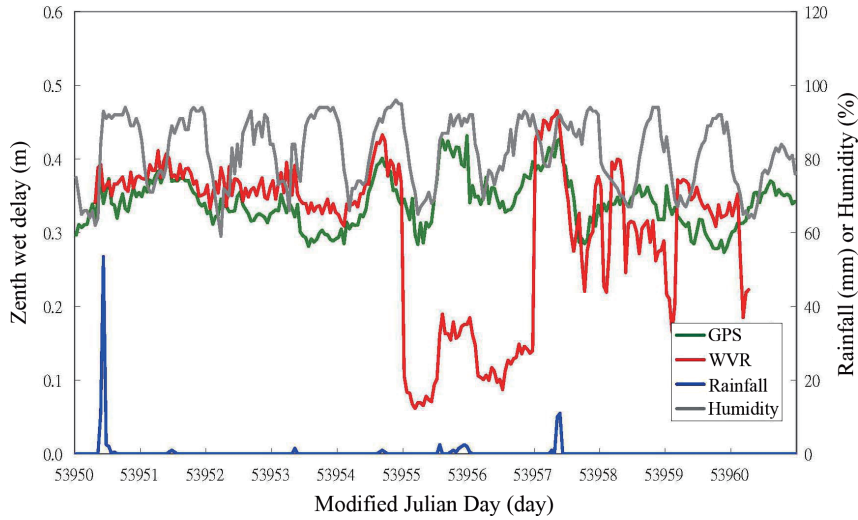


Fig. 7. The GPS-ZWD, WVR-ZWD, relative humidity, and precipitation data from station PKGM during the typhoon period.

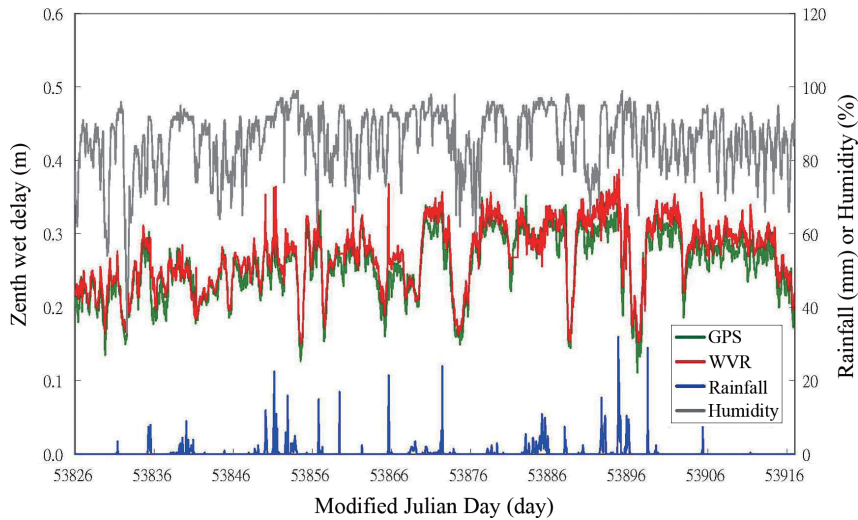


Fig. 8. The GPS-ZWD, WVR-ZWD, relative humidity, and precipitation data from station YMSM during the long-duration case.

measured by the WVR and ZWD calculated from GPS displayed the same trend. The correlation coefficient was 0.94, and the average difference was 1.26 cm. Both of these parameters were better than those for the typhoon case, but slightly worse than those of the plum rain season case. By comparing the precipitation and the ZWD, we found that the delay increases dramatically whenever rainfall occurs, whereas the wet delay decreases rapidly following rainfall.

Figure 9 shows the results for station PKGM. During the period from April to June, the majority of the precipitation occurred in June in southern Taiwan. The correlation coefficient between the WVR-ZWD and GPS-ZWD measurements was 0.91, and the average difference was 1.89 cm. This result is better than those for the two short-duration cases. Compared with the typhoon case, the improved results in the long-duration case may be caused by the low

GPS accuracy, which resulted from the severe change that occurred in the atmosphere during the typhoon period. In the plum rain case, station PKGM was located in an area that experienced torrential rainfall (the hourly precipitation was 20 - 60 mm). Therefore, the inaccuracies could be attributed to the larger observational errors in WVR.

After verifying the precipitable water vapor that was calculated from the GPS data using the WVR data, we further analyzed the relationship between ZWD and precipitation, by dividing the long-duration data into two types: those with and without precipitation (see Table 1). We also separated the stations into flatland and mountain stations. The stations were then ranked according to their latitudes. Table 1 shows that the ZWD threshold of precipitation for the flatland stations was 0.36 m, whereas it was only 0.31 m for the mountain stations. This is a difference of 0.05 m,

which represents 14% of the total. The same phenomenon was observed in the data without precipitation. The average ZWDs of the flatland stations and mountain stations were 0.31 and 0.27 m, respectively. The difference was 0.04 m,

which represents 13% of the total. Therefore, the height of the station must be considered when using ZWD to predict whether rainfall will occur. The reasoning is as follows. Because the mountain station is located at a higher altitude,

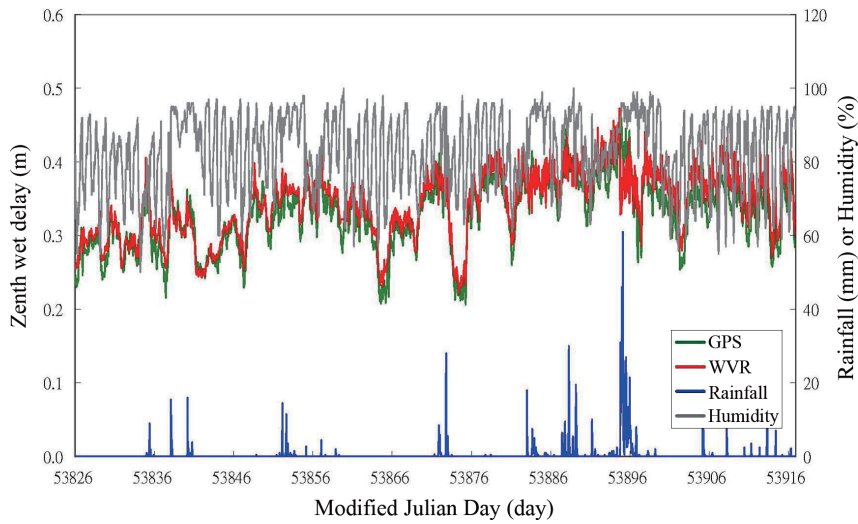


Fig. 9. The GPS-ZWD, WVR-ZWD, relative humidity, and precipitation data from station PKGM during the long-duration case.

Table 1. The average ZWD with and without rainfall from the flatland and mountain stations.

Flatland station	Latitude	Height (m)	With rainfall ZWD (m)	Without rainfall ZWD (m)
MZUM	26°09'N	60	0.35	0.28
GS10	25°08'N	52	0.35	0.31
SHJU	24°50'N	24	0.36	0.31
YILN	24°44'N	64	0.35	0.32
KMNM	24°24'N	49	0.37	0.31
TACH	24°17'N	34	0.37	0.32
CAOT	23°58'N	142	0.37	0.31
SOFN	23°52'N	59	0.37	0.32
PKGM	23°34'N	43	0.38	0.32
TMAM	22°37'N	59	0.37	0.31
KDMN	21°57'N	58	0.37	0.32
<b>Average</b>		<b>59</b>	<b>0.36</b>	<b>0.31</b>
<b>Standard deviation</b>			<b>0.010</b>	<b>0.012</b>
Mountain station	Latitude	Height (m)	With rainfall ZWD (m)	Without rainfall ZWD (m)
YMSM	25°10'N	784	0.29	0.25
SINY	23°41'N	536	0.33	0.28
LANB	22°02'N	351	0.32	0.28
<b>Average</b>		<b>557</b>	<b>0.31</b>	<b>0.27</b>
<b>Standard deviation</b>			<b>0.021</b>	<b>0.017</b>

the region of the troposphere through which the GPS signal passes to reach the GPS receivers is thinner for the mountain station than for the flatland station. Therefore, the error in position due to the water vapor delay is smaller. Conversely, the GPS signals must pass through a thicker layer of troposphere before reaching the flatland stations. Therefore, the signal delay effect at the flatland stations is larger than that at the mountain stations.

Next, we divided the data into heavy rain, moderate rain, and light rain categories to investigate the correlation between ZWD and the rainfall strength (Table 2). The definitions of the three categories are as follows: heavy rain refers to rainfall with an hourly precipitation rate above 20 mm, moderate rain refers to rainfall with an hourly precipitation rate between 10 and 20 mm, and light rain refers to rainfall with an hourly precipitation rate of less than 10 mm. Table 2 shows that when light rain occurred at the flatland stations, the average ZWD was 0.36 m; when moderate rain occurred, the average ZWD increased to 0.38 m. The difference was 0.02 m, which represents 5% of the total. When heavy rain occurred, the average ZWD reached 0.40 m. The difference between the heavy rain and moderate rain was 0.02 m, which represents 5% of the total. When light rain, moderate

rain, and heavy rain occurred at the mountain stations, the corresponding ZWD values were 0.30, 0.33, and 0.34 m, respectively. The increase was only slightly different than that at the flatland stations. Based on the aforementioned results, we concluded that at regions with different elevations, the GPS-ZWD values cannot be used alone to decide whether a potential for precipitation exists; the estimates of GPS-ZWD should also be used to decide the strength of the precipitation. Recently, the CWB has applied ground-based GPS to calculate near real-time ZWD data. By importing these data into the numerical meteorological model, encouraging preliminary results have been obtained (Bevis et al. 1992; Rocken et al. 1993; Liou and Huang 2000). If this method can be applied to all 400+ GPS stations in Taiwan and its surrounding islands, higher spatial- and temporal-resolution data can be provided to the city and countryside weather-forecast system currently under development. Consequently, the quality of the fundamental information that is used in weather forecasting can be improved.

## 5. CONCLUSIONS AND RECOMMENDATIONS

In this study, we utilized ground-based GPS signals and

Table 2. The average ZWD during different rainfall strengths from the flatland and mountain stations.

Flatland station	Latitude	Height (m)	Light rain ZWD (m)	Moderate rain ZWD (m)	Heavy rain ZWD (m)
MZUM	26°09'N	60	0.36	0.37	0.38
GS10	25°08'N	52	0.35	0.38	0.40
SHJU	24°50'N	24	0.36	0.37	0.40
YILN	24°44'N	64	0.35	0.39	0.40
KMNM	24°24'N	49	0.37	0.38	0.38
TACH	24°17'N	34	0.37	0.39	0.40
CAOT	23°58'N	142	0.36	0.39	0.39
SOFN	23°52'N	59	0.36	0.42	0.40
PKGGM	23°34'N	43	0.38	0.39	0.42
TMAM	22°37'N	59	0.37	0.39	0.42
KDMN	21°57'N	58	0.36	0.36	0.41
<b>Average</b>		<b>59</b>	<b>0.36</b>	<b>0.38</b>	<b>0.40</b>
<b>Standard deviation</b>			<b>0.009</b>	<b>0.016</b>	<b>0.013</b>
Mountain Station	Latitude	Height (m)	Light rain ZWD (m)	Moderate rain ZWD (m)	Heavy rain ZWD (m)
YMSM	25°10'N	784	0.28	0.31	0.31
SINY	23°41'N	536	0.32	0.34	0.36
LANB	22°02'N	351	0.31	0.33	0.36
<b>Average</b>		<b>557</b>	<b>0.30</b>	<b>0.33</b>	<b>0.34</b>
<b>Standard deviation</b>			<b>0.021</b>	<b>0.015</b>	<b>0.029</b>

surface temperature measurements to calculate the ZWD values. The accuracy of the GPS-ZWD data was verified using the ZWD that was measured by the WVR. Based on the averaged data from stations YMSM and PKGM, the difference between the GPS-ZWD and WVR-ZWD estimates was 1.31 cm in the plum rain season case. The correlation coefficient was 0.93. In the typhoon case, the difference between the GPS-ZWD and WVR-ZWD values was 2.57 cm, and the correlation coefficient was 0.89. In the long-duration case, the difference between the GPS-ZWD and WVR-ZWD estimates was 1.58 cm, and the correlation coefficient was 0.93. Assuming that WVR-ZWD is correct to evaluate the accuracy of GPS-ZWD values, we observed only minimal differences between the long-duration and plum rain season cases. However, the accuracy obtained during the typhoon case was notably reduced. This reduction could be related to the 1-hr resolution of the ZWD data. In other words, we assumed that the ZWD values do not change significantly over the course of an hour. However, because atmospheric parameters can change rapidly during a typhoon period, ZWD cannot be a fixed value. Therefore, the accuracy of the GPS-ZWD data was lower in the typhoon case. In the future, 30- or even 15-min time sampling may be used to calculate the ZWD. However, a higher time resolution may also produce too many unknowns, which may lead to an unsolvable problem or to decreased accuracy. Moreover, although the WVR is equipped with the Rain Effect Mitigation component, the observational data derived from the WVR were notably abnormal when the rate of rainfall was greater than 20 mm hr<sup>-1</sup>. This phenomenon could be related to the measurement error caused by the water drops adhering to the surface of WVR during periods of heavy rainfall. Therefore, during heavy rainfall, GPS data are more reliable than WVR data.

In this study, we also observed that rainfall can occur at flatland stations when the average ZWD value reaches 0.36 m; at mountain stations, this value is 0.31 m. The difference between the values is 0.05 m, which represents 14% of the total. Therefore, the height of the station must be considered when the ZWD is used to decide whether a certain area will experience rainfall. Furthermore, when the flatland stations experienced light rain, moderate rain, and heavy rain, the ZWDs were 0.36, 0.38, and 0.40 m, respectively. For the mountain stations, the ZWDs were 0.30, 0.33, and 0.34 m, respectively. This result suggests that at different elevations, the ZWD value can be used to forecast the potential for and strength of precipitation. The GPS calculation method that was used in this study, long baseline static relative positioning, was used to eliminate many common system errors. Although this method can generate a higher accuracy for the ZWD calculation, the accuracy greatly depends on the reference station. In the future, if the Precise Point Positioning (PPP) method can be revised to improve the accuracy of the error correction, absolute and independent ZWD values can

be obtained; this goal will be the focus of our future studies.

**Acknowledgments** The authors would like to thank the National Science Council of the Republic of China, Taiwan, for financially supporting this research under Contract No. NSC 99-2111-M-305-001-MY3.

## REFERENCES

- Aguado, E. and J. E. Burt, 2009: Understanding Weather and Climate, Fifth edition, Prentice Hall, 608 pp.
- Bevis, M., S. Businger, T. A. Herring, C. Rocken, R. A. Anthes, and R. H. Ware, 1992: GPS meteorology: Remote sensing of atmospheric water vapor using the global positioning system. *J. Geophys. Res.*, **97**, 15787-15801, doi: 10.1029/92jd01517. [[Link](#)]
- Bevis, M., S. Businger, S. Chiswell, T. A. Herring, R. A. Anthes, C. Rocken, and R. H. Ware, 1994: GPS meteorology: Mapping zenith wet delays onto precipitable water. *J. Appl. Meteorol.*, **33**, 379-386, doi: 10.1175/1520-0450(1994)033<0379:gmmzwd>2.0.co;2. [[Link](#)]
- Bock, O. and E. Doerflinger, 2001: Atmospheric modeling in GPS data analysis for high accuracy positioning. *Phys. Chem. Earth Solid Earth Geodes.*, **26**, 373-383, doi: 10.1016/s1464-1895(01)00069-2. [[Link](#)]
- Chen, C. H., T. K. Yeh, J. Y. Liu, C. H. Wang, S. Wen, H. Y. Yen, and S. H. Chang, 2011: Surface deformation and seismic rebound: Implications and applications. *Surv. Geophys.*, **32**, 291-313, doi: 10.1007/s10712-011-9117-3. [[Link](#)]
- Chen, G. and T. A. Herring, 1997: Effects of atmospheric azimuthal asymmetry on the analysis of space geodetic data. *J. Geophys. Res.*, **102**, 20489-20502, doi: 10.1029/97jb01739. [[Link](#)]
- CWB, 2011: Webpage of Center Weather Bureau. Available at <http://www.cwb.gov.tw/>.
- Davis, J. L., T. A. Herring, I. I. Shapiro, A. E. E. Rogers, and G. Elgered, 1985: Geodesy by radio interferometry: Effects of atmospheric modeling errors on estimates of baseline length. *Radio Sci.*, **20**, 1593-1607, doi: 10.1029/rs020i006p01593. [[Link](#)]
- Emardson, T. R., G. Elgered, and J. M. Johansson, 1998: Three months of continuous monitoring of atmospheric water vapor with a network of Global Positioning System receivers. *J. Geophys. Res.*, **103**, 1807-1820, doi: 10.1029/97jd03015. [[Link](#)]
- Ifadis, I. M. and P. Savvaiddis, 2001: Space to earth geodetic observations: Approaching the atmospheric effect. *Phys. Chem. Earth Solid Earth Geodes.*, **26**, 195-200, doi: 10.1016/s1464-1895(01)00046-1. [[Link](#)]
- Kueh, M. T., C. Y. Huang, S. Y. Chen, S. H. Chen, and C. J. Wang, 2009: Impact of GPS radio occultation refractivity soundings on a simulation of Typhoon Bilis (2006) upon landfall. *Terr. Atmos. Ocean. Sci.*, **20**,

- 115-131, doi: 10.3319/tao.2008.01.21.03(F3C). [[Link](#)]
- Leick, A., 2004: GPS Satellite Surveying, John Wiley and Sons, New Jersey, 435 pp.
- Liou, Y. A. and C. Y. Huang, 2000: GPS observations of PW during the passage of a typhoon. *Earth Planets Space*, **52**, 709-712.
- Liou, Y. A., C. Y. Huang, and Y. T. Teng, 2000: Precipitable water observed by ground-based GPS receivers and microwave radiometry. *Earth Planets Space*, **52**, 445-450.
- Liou, Y. A., Y. T. Teng, T. van Hove, and J. C. Liljegren, 2001: Comparison of precipitable water observations in the near tropics by GPS, microwave radiometer, and radiosondes. *J. Appl. Meteorol.*, **40**, 5-15, doi: 10.1175/1520-0450(2001)040<0005:copwoi>2.0.co;2. [[Link](#)]
- Mendes, V. B. and R. B. Langley, 1999: Tropospheric zenith delay prediction accuracy for high-precision GPS positioning and navigation. *J. Inst. Navig.*, **46**, 25-33.
- Niell, A. E., 1996: Global mapping functions for the atmosphere delay at radio wavelengths. *J. Geophys. Res.*, **101**, 3227-3246, doi: 10.1029/95jb03048. [[Link](#)]
- NOAA, 2013: Webpage of National Oceanic and Atmospheric Administration. Available at <http://www.noaa.gov/>.
- Rocken, C., R. Ware, T. van Hove, F. Solheim, C. Alber, J. Johnson, M. Bevis, and S. Businger, 1993: Sensing atmospheric water vapor with the Global Positioning System. *Geophys. Res. Lett.*, **20**, 2631-2634, doi: 10.1029/93gl02935. [[Link](#)]
- Ruddiman, W. F., 2007: Earth's Climate: Past and Future, Second edition, W. H. Freeman, 465 pp.
- Solheim, F. S., J. Vivekanandan, R. H. Ware, and C. Rocken, 1999: Propagation delays induced in GPS signals by dry air, water vapor, hydrometeors, and other particulates. *J. Geophys. Res.*, **104**, 9663-9670, doi: 10.1029/1999jd900095. [[Link](#)]
- Solomon, S., 2011: Water: The Epic Struggle for Wealth, Power, and Civilization, Harper Perennial, 624 pp.
- Shoji, Y., 2009: A study of near real-time water vapor analysis using a nationwide dense GPS network of Japan. *J. Meteorol. Soc. Jpn.*, **87**, 1-18, doi: 10.2151/jmsj.87.1. [[Link](#)]
- Tregoning, P., R. Boers, D. O'Brien, and M. Hendy, 1998: Accuracy of absolute precipitable water vapor estimates from GPS observations. *J. Geophys. Res.*, **103**, 28701-28710, doi: 10.1029/98jd02516. [[Link](#)]
- Yeh, T. K., C. S. Wang, C. W. Lee, and Y. A. Liou, 2006: Construction and uncertainty evaluation of a calibration system for GPS receivers. *Metrologia*, **43**, 451-460, doi: 10.1088/0026-1394/43/5/017. [[Link](#)]
- Yeh, T. K., Y. A. Liou, C. S. Wang, and C. S. Chen, 2008: Identifying the degraded environment and bad receivers setting by using the GPS data quality indices. *Metrologia*, **45**, 562-570, doi: 10.1088/0026-1394/45/5/010. [[Link](#)]
- Yeh, T. K., C. Hwang, J. F. Huang, B. F. Chao, and M. H. Chang, 2011: Vertical displacement due to ocean tidal loading around Taiwan based on GPS observations. *Terr. Atmos. Ocean. Sci.*, **22**, 373-382, doi: 10.3319/tao.2011.01.27.01(T). [[Link](#)]
- Yeh, T. K., Y. D. Chung, C. T. Wu, C. S. Wang, K. Zhang, and C. H. Chen, 2012: Identifying the relationship between GPS data quality and positioning precision: Case study on IGS tracking stations. *J. Surv. Eng.*, **138**, 136-142, doi: 10.1061/(ASCE)SU.1943-5428.0000077. [[Link](#)]
- Yeh, T. K., C. H. Chen, G. Xu, C. S. Wang, and K. H. Chen, 2013: The impact on the positioning accuracy of the frequency reference of a GPS receiver. *Surv. Geophys.*, **34**, 73-87, doi: 10.1007/s10712-012-9202-2. [[Link](#)]